Catena 198 (2021) 105047

Contents lists available at ScienceDirect

Catena

journal homepage: www.elsevier.com/locate/catena

Contrasting responses of soil C-acquiring enzyme activities to soil erosion and deposition

Lanlan Du [a,b], Rui Wang [c], Yaxian Hu [c], Xiaogang Li [c], Sheng Gao [c], Xihui Wu [c], Xin Gao [c], Lunguang Yao [d], Shengli Guo [a,b,c,d,*]

[a] State Key Laboratory of Soil Erosion and Dryland Farming on the Loess Plateau, Institute of Soil and Water Conservation, Chinese Academy of Sciences and Ministry of Water Resources, Yangling, Shaanxi 712100, China
[b] University of Chinese Academy of Sciences, Beijing 100049, China
[c] Institute of Soil and Water Conservation, Northwest A&F University, Yangling, Shaanxi 712100, China
[d] Collaborative Innovation Center of Water Security for Water Source, Region of Mid-line of South-to-North Diversion Project of Henan Province, Nanyang Normal University, Nanyang, Henan 473061, China

ARTICLE INFO

Keywords:
Erosional plot
Depositional plot
Soil CO_2 emission
Chinese Loess Plateau

ABSTRACT

Soil C-acquiring enzymes are good indicators for the biological mechanism of soil nutrients and organic matter cycles. However, they have been used less frequently to assess the ecological stability and soil C cycle in eroding landscapes due to a lack of knowledge of the responses of C-acquiring enzyme activities to soil erosion and deposition. In the present study, a 3-year field simulation experiment was conducted to examine the variations in the activities of C-acquiring enzymes (β-1,4-xylosidase (βX), β-1,4-glucosidase (βG) and β-D-cellobiohydrolase (CBH)) from erosion-deposition plots with different slope gradients (5°, 10° and 20°) on the Loess Plateau in China (2016–2018). The activities of βX, βG and CBH were higher in the depositional plots than in the erosional plots, and those differences were enlarged with increasing slope gradients. Compared to the 5°-erosional plot, the activities of βX, βG and CBH respectively declined by 3.2–4.5%, 14.3–37.5% and 12.7–29.1% in the 10°-and 20°-erosional plots. The βX, βG and CBH activities were 2.2–18.1%, 17.3–32.1% and 14.8–86.2% higher in the 10°- and 20°-depositional plots than in the 5°-depositional plot. Moreover, the total soil CO_2 emissions from the whole erosion-deposition plots decreased as slopes steepened. The displaced runoff and sediment depleted soil moisture, SOC, clay and microbial biomass in the erosional plots but enhanced these resources in the depositional plots, which can account for the changes in C-acquiring enzyme activities. The spatial distribution of enzyme activities affected soil CO_2 emissions in a positive linear function. The sensitive responses of the C-acquiring enzyme activities and the controlling effects of C-acquiring enzyme activities on soil CO_2 emissions during erosion and deposition processes, should be properly considered in assessing the biological mechanism for nutrition cycling in regions predominated with fragmented eroding landscapes.

1. Introduction

Soil erosion and deposition, as the engine to redistribute soil from land surfaces and to influence the biogeochemical cycling of essential soil elements, are phenomena observed globally (Berhe et al., 2018; de Nijs and Cammeraat, 2020; Kuhn et al., 2009; Lal, 2019). Annually, water erosion is estimated globally to redistribute 1–5 Pg carbon (C) (Mccarty and Ritchie, 2002; Stallard, 1998; Starr et al., 2001), accompanied by the delivery of soil moisture, nutrients, particles and microorganisms from eroding sites to depositional sites (Du et al., 2020; Hu and Kuhn, 2016; Polyakov and Lal, 2008; Wei et al., 2016; Xiao et al., 2018). Soil C-acquiring enzymes are important components in soil biochemical processes, which are crucial in catalysing the soil C cycle (Peng and Wang, 2016; Sinsabaugh et al., 2008; Xu et al., 2017). The activities of soil C-acquiring enzymes are highly variable due to environmental variables including soil texture (Tietjen and Wetzel, 2003), substrate availability (Sinsabaugh et al., 2008) and soil moisture (Alster et al., 2013). It is reasonable to assume that soil erosion- and deposition-induced spatial variations in hydrologic, pedologic and microclimatic conditions are predicted to influence the activities of soil C-acquiring enzymes. Such changes in soil C-acquiring enzymes could potentially perturb the catalysing and mediating functions of the soil C-acquiring

* Corresponding author at: Institute of Soil and Water Conservation, Xinong Road 26, Yangling, Shaanxi 712100, China.
E-mail address: guoshli@nwafu.edu.cn (S. Guo).

https://doi.org/10.1016/j.catena.2020.105047
Received 16 May 2020; Received in revised form 14 October 2020; Accepted 9 November 2020
Available online 16 November 2020

enzymes in ecological processes. However, there is little knowledge on the responses of soil C-acquiring enzymes to soil erosion and deposition. Therefore, some uncertainties were remained in researching the mechanism of biogeochemical processes shifts and ecosystem stability in eroding landscapes.

Several studies have addressed the changes in soil enzyme activities subjected to erosion and deposition. Soil enzyme activities are suppressed by erosion while being enhanced by deposition, which related to the depleted SOC, soil moisture and microbial biomass in the eroding sites and the enrichment of those resources in the depositional sites (Li et al., 2015; Moreno-de las Heras, 2009; Nie et al., 2015; Park et al., 2014; Sarapatka et al., 2018). Of the previous studies above, only Moreno-de las Heras (2009) has researched the soil C-acquiring enzyme activities in slope lands and demonstrated that the activity of β-1,4-glucosidase (βG) was exponentially reduced when erosion exacerbated the deficiency in available resources (Moreno-de las Heras, 2009). The other soil C-acquiring enzyme activities including β-D-cellobiohydrolase (CBH) and β-1,4-xylosidase (βX) have been not investigated for their responses to soil erosion. Actually, soil C-acquiring enzyme activities do not respond consistently to altered soil conditions. For instance, the βG and CBH sorbed to clay particles present low activities (Allison and Jastrow, 2006) or can still be chemically active, but the βX adsorption produces enhanced enzyme activities (Tietjen and Wetzel, 2003). A study across seven biogeoclimatic zones declares that the activity of βG is negatively related to the soil moisture, but the activities of βX and CBH are not (Brockett et al., 2012). Accompanied by the intense and complex variations of soil physicochemical and microbial properties, soil erosion may complicate the responses of three C-acquiring enzyme activities to soil factors. It is necessary to confirm whether the responses of the activities of βX and CBH to soil erosion is consistent with that of the activity of βG. Furthermore, it is unclear the effect that deposition has on soil C-acquiring enzyme activities. Deposition generally occurs when soil erosion happened and is accompanied by changeable runoff, sediment and soil nutrients (Park et al., 2014; Sagova-Mareckova et al., 2016).

The C-acquiring enzymes are crucial for the functioning of the rate-limiting step of SOC depolymerization (Ali et al., 2018; Burns et al., 2013; Conant et al., 2011; Sinsabaugh et al., 2008). A considerable proportion of heterotrophic respiration is controlled by enzyme activities (Ali et al., 2015; Ali et al., 2018). The changeable soil C-acquiring enzymes during the processes of soil detachment, transportation and deposition would perturb soil CO_2 emissions in the eroding landscape and further alter the soil C sequestration in terrestrial ecosystems. Therefore, the study of the effects of soil C-acquiring enzyme activities on soil CO_2 emissions during soil erosion and deposition can help to distinguish the uncertainty in the erosion- and deposition-induced soil C source or sink (Lal, 2019; Van Oost et al., 2007).

In this study, erosion–deposition plots including the erosional plots with three gradients (5°, 10° and 20°) and the depositional plots, were systematically conducted on the Loess Plateau, China. Through observing soil C-acquiring enzyme activities, runoff and sediment, we aimed to (1) identify the responses of the soil C-acquiring enzyme activities to soil erosion and deposition and (2) investigate the effects of the soil C-acquiring enzyme activities on soil CO_2 emissions in the erosion–deposition plots.

2. Materials & methods

2.1. Site description and experimental design

The study site was established at the Wangdong catchment (35°13′ N, 107°40′ E, altitude 1220 m), Changwu, southern Loess Plateau, China. The mean annual precipitation was approximately 560 mm, with 60% of the rainfall occurring in the period from July to September, and the mean annual air temperature was 9.4 °C (provided by the Shaanxi Changwu Agroecosystem National Observation and Research Station). The local soil is dominated by loam (Cumulic Haplustoll; the USDA Soil Taxonomy System), which originated from the Loess deposits. The local landscape is characterized by tableland (remnant flat parts of the plateau), slopes (or gullies) and valley bottoms. The relatively flat tableland with a gradient <5°, covers 38% of the total area and has a low erosion rate of <100 t km^{-2} y^{-1}. The slope lands with ranging from 5° to 50° are the main erosional areas, covering 53% of the total area and eroding at a rate 100–20,000 t km^{-2} y^{-1}. The valley bottom (gradient < 10°) receives the eroded materials from the tableland and the slopes (Wang et al., 2017).

To simulate the local eroding landscape, a set of erosion–deposition plots with east-facing and replicating three times (Fig. 1a, b, c), were constructed in April 2014. Detailed information on the erosion–deposition plots, soil preparation and management has been described in Du et al. (2020). In brief, the erosion–deposition plots of three slope gradients (5°, 10° and 20°) were constructed and refilled with 200 cm-deep soil collected from local farmland. Each plot included an erosional plot (500 cm long × 100 cm wide × 200 cm deep) and a connected depositional plot (100 cm long × 100 cm wide × 200 cm deep). The erosional plots across three slope gradients (5°, 10° and 20°) have been defined as 5°-erosional plot, 10°-erosional plot and 20°-erosional plot. In meanwhile, the depositional plots connected with the erosional plots across three slope gradients have been defined as 5°-depositional plot, 10°-depositional plot and 20°-depositional plot.

A fourth replicate, marked by the dotted yellow lines in Fig. 1a, b, was built for each slope gradient to monitor runoff and sediment during the individual rainfall. Patterns of runoff and sediment from different slopes have been found to be reasonably consistent over 43 individual erosion events during the experimental period of 2016–2018 (Table S1). This has confirmed the controlling effects of the slope gradients on the erosion processes. Thus it proved that one replicate to monitor soil erosional responses was adequate to examine the responses of soil enzyme activities to runoff and sediment displacement. Moreover, considering the prevalence of the gentle slopes on the tableland of the Loess Plateau (Wang et al., 2017), the 5° erosion–deposition plots were set as the reference plots in this study.

2.2. Runoff and sediment collection

After each detectable erosion event, the runoff suspension was immediately collected into a cylindrical steel tank placed at the lower end of each monitored erosional plot. After recording the suspension weight and volume, three well-blended suspension subsamples, 500 mL each, were re-sampled from each tank and air-dried to calculate the sediment concentration. For more detailed information on the runoff and sediment collection and calculation, please refer to Du et al. (2020).

2.3. Sampling and measuring the soil properties

During the experimental period (2016–2018), the sediment in each depositional plot was left to natural deposition. At the end of each experimental year, the accumulated sediment depths in the 5°-, 10°- and 20°-depositional plots were measured, and the results were listed in Table S2. The sediment depth exhibited variations between three slope gradients. Soil samples from the same depth were collected from each erosional and depositional plot, which can help us to solely examine the responses of soil C-acquiring enzyme activities to soil erosion and deposition, rather than involving the spatial variations in soil conditions intrinsic to soil depth. At the end of each experimental year (end of November in 2016, 2017, and 2018), the five soil cores, from 0 to 10 cm deep, were randomly collected from each erosional and depositional plot. Each soil core was collected using a 3 cm auger and then mixed to form composite samples. Every composite soil sample was then divided into two parts: one part was air-dried to determine the soil physicochemical properties, and the other part was preserved at 4 °C for assays of soil microbial biomass, and soil C-acquiring enzyme activities.

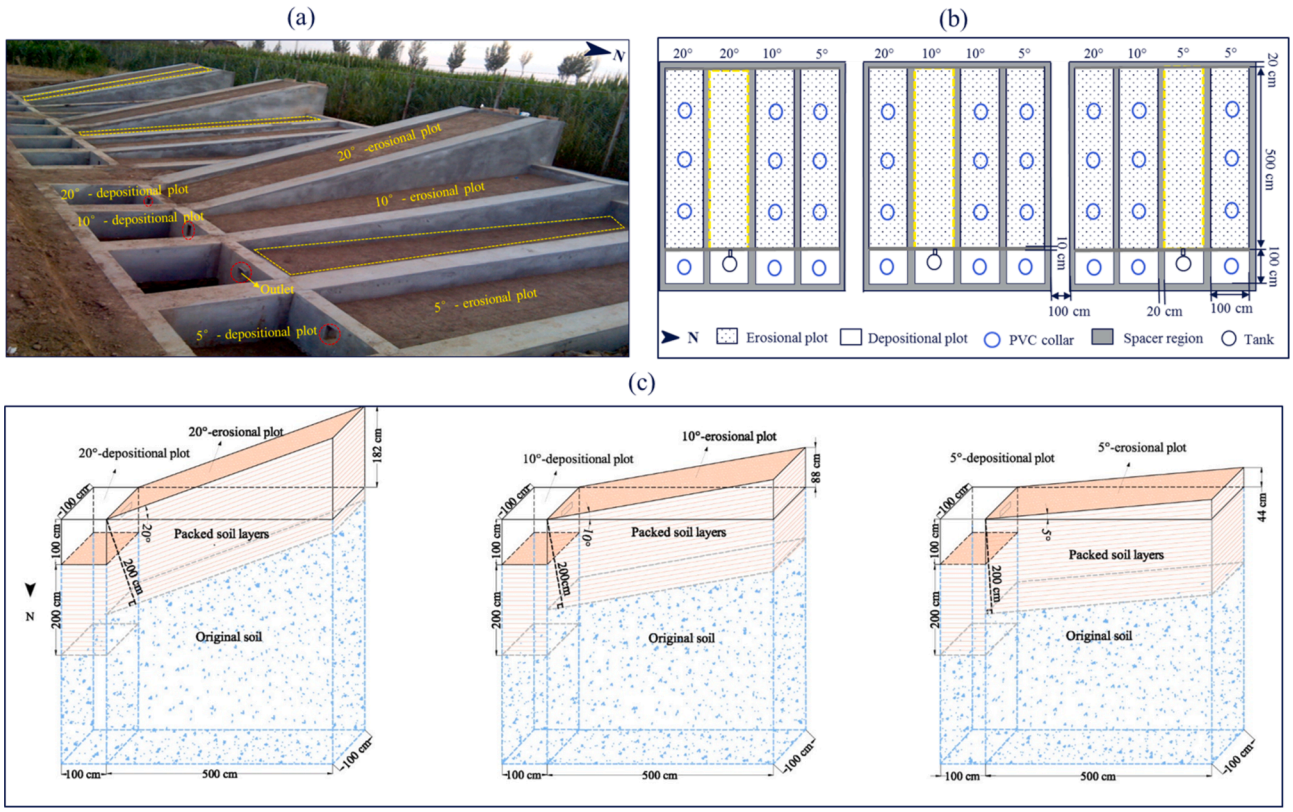

Fig. 1. Experimental set-up. (a) Photograph of the field experimental settings; (b) layout of the experimental settings of the erosional plots and the depositional plots across three slope gradients; (c) detailed design of the profiles of the erosional plots and the depositional plots across three slope gradients (cited from Du et al. (2020)).

Soil physicochemical properties and their assay methods in this study have been summarized in Table 1. In detail, soil samples were extracted with 60 mL of 0.5 mol K_2SO_4 to measure the DOC content. The NO_3-N, and NH_4-N were extracted with KCl (1 mol L^{-1}), then their sum was defined as the mineral nitrogen (N_{min}) in this study. The MBC and MBN were determined with conversion factors K_C of 0.38 for MBC and K_N of 0.45 for MBN respectively. According to the description outlined by Zhang et al. (2015), soil CO_2 emission rate was regularly monitored approximately every 10 days from April 2016 to November 2018.

Table 1
Summary of soil physicochemical properties and their assay methods in this study.

Soil physicochemical properties	Abbreviation	Assay method
Soil gravimetric moisture	Soil moisture	Oven-dried at 105 °C for 12 h to achieve a constant weight
Soil clay (<0.002 mm)	Clay	Using Mastersizer 2000 (Malvern Instruments Ltd., Worcestershire, UK)
Soil bulk density	BD	Cutting ring (Grossman and Reinsch, 2002)
Soil organic carbon	SOC	K_2CrO_7-H_2SO_4 oxidation (Sparks et al., 1996)
Soil dissolved organic carbon	DOC	Using a total organic carbon analyzer (TOC-VCSH, Shimadzu, Japan)
Soil total nitrogen	TN	Kjeldahl method (Kjeldahl, 1883)
Soil nitrate nitrogen/ ammonium nitrogen	NO_3-N/ NH_4-N	Analyzed by an Auto Analyzer III continuous flow instrument (Bran + Luebbe GmbH, Germany)
Soil microbial biomass carbon/ nitrogen	MBC/ MBN	Chloroform fumigation-extraction (Vance et al., 1987; Brookes et al., 1985)
Soil carbon dioxide emission rate	Soil CO_2 emission rate	Measured by an automated closed soil CO_2 flux system equipped with a portable chamber (20 cm in diameter; Li-8100, Lincoln, NE, USA)

2.4. Assays of soil C-acquiring enzyme activities

The activities of β-1,4-xylosidase (βX), β-1,4-glucosidase (βG) and β-D-cellobiohydrolase (CBH) were measured fluorometrically using a 200 μM solution of substrates labelled with 4-methylumbelliferone (MUB), according to the method outlined in Saiya-Cork et al. (2002). The soil suspension was prepared by adding 1 g fresh soil from each erosional and depositional plot to 125 mL of 50 mM buffer, followed by homogenization for 2 h in a constant temperature shaker. The prepared suspensions were continuously stirred while 200 μl aliquots were dispensed into the 96-well microplates. The details for the preparation of the samples, blank, quench, reference standard and negative control are as follows: 50 μl of 200 μM substrate solution was added to 200 μl of the sample suspension for each sample well; 50 μl of buffer was added to 200 μl of sample suspension for the blank wells; 50 μl of standard (10 μM 4-methylumbelliferone-MUB) was added to 200 μl sample suspension for each quench well; 50 μl of substrate solution was added to 200 μl of buffer for the negative control wells; 50 μl of standard was added to 200 μl acetate buffer for the reference standard wells. The prepared plates were incubated in the dark at 25 °C for 4 h. To stop the reaction, 50 μl of 0.5 M NaOH was added to each well after incubation. The fluorescence was measured using a microplate reader (SpectraMax Gemini, Molecular Devices, CA, USA) at excitation and emission wavelengths of 365 nm and 450 nm, respectively. The soil C-acquiring enzyme activities were corrected for quench and negative controls and expressed in units of nmol activity per hour per gram of dry soil (nmol g^{-1} dry soil h^{-1}).

2.5. Statistical analysis

The mean daily soil CO_2 emission rate was interpolated between the measurement dates, the daily cumulative CO_2 emission rate calculated as following:

$$CR_s = R_s \times 3600 \times 24 \times 12/10^6 \quad (1)$$

where CR_S is the daily cumulative soil CO_2 emission rate (g CO_2-C m^{-2}); R_s is the average soil CO_2 emissions rate (μ mol m^{-2} s^{-1}) at each measurement; 3600 and 24 are the conversion coefficient of time; 12 is the molar mass of C (g mol^{-1}); 10^6 is the conversion coefficient between micromoles and moles.

The yearly cumulative soil CO_2 emission was calculated by summing up the daily cumulative CO_2 emission rate during April to November of each experimental year.

The total soil CO_2 emissions from the erosion–deposition plots of 5°, 10° and 20° slopes were then calculated as following:

$$R_{t-i} = R_{Ero} \times A_{Ero} + R_{Dep} \times A_{Dep} \quad (2)$$

where $R_{t\text{-}i}$ is the total soil CO_2 emission (g CO_2-C y^{-1}) in the erosion–deposition plots under different slope gradients (i represents slope gradient as 5°, 10° or 20°); R_{Ero} is the yearly cumulative soil CO_2 emission from a unit area in the erosional plots (g CO_2-C m^{-2} y^{-1}); R_{Dep} is the yearly cumulative soil CO_2 emission from a unit area in the depositional plots (g CO_2-C m^{-2} y^{-1}); the A_{Ero} and A_{Dep} are the areas (m^2) of the erosional plot and the depositional plot, and their respective values are 5 m^2 and 1 m^2 in this experiment.

The differences in the soil C-acquiring enzyme activities and environmental factors among the 5°-, 10°- and 20°- erosional plots and their depositional plots (mean ± SD, n = 3) were compared by analysis of variance (ANOVA) and a Duncan test at a probability of 5% ($p = 0.05$) using the software program SPSS ver. 20.0 (SPSS Inc., Chicago, IL, USA). Relationships between runoff and sediment, soil properties and soil C-acquiring enzyme activities were tested and quantified using structural equation modelling (SEM) method in IBM SPSS Amos ver. 23.0. To test for goodness of fit of the model, the non-significant chi-square (χ^2) test (the model has a good fit when $0 \le \chi^2 \le 2$ and $0.05 < p \le 1.00$) and the root mean square error of approximation (RMSEA, the model has a good fit when $0 \le$ RMSEA ≤ 0.05 and $0.10 < p \le 1.00$) were used according to Delgado-Baquerizo et al. (2015).

3. Results

3.1. Soil biogeochemical properties in the erosional and the depositional plots

During the experimental period of 2016–2018, the annual runoff and sediment yield generated on the 5° slopes were 0.23–0.30 m^3 and 2–14 kg, respectively, which increased by 30–207% and 157–780% on the steeper slopes of 10° and 20°, respectively, compared to the 5° slopes (Table 2).

The soil physical and biochemical properties presented divergent redistributions in the erosional and the depositional plots (Table 3). During the experimental period (2016–2018), the contents of N_{min}, soil moisture, MBC, MBN and clay in the depositional plots were higher than that in the erosional plots ($p < 0.05$, Table 3). When compared to the 5°-erosional plots, soil moisture, MBC and MBN decreased in the 10°- and 20°-erosional plots. In contrast, soil moisture, MBC and MBN increased in the 10°- and 20°-depositional plots compared to that in the 5°-depositional plots (Table 3).

3.2. Soil C-acquiring enzyme activities in the erosional and the depositional plots

The soil C-acquiring enzyme activities presented different spatial variations in the erosional and depositional plots. Significantly, the activities of soil C-acquiring enzymes were higher in the depositional plots than that in the erosional plots ($p < 0.05$, Fig. 2). When compared to the 5°-erosional plots, the enzyme activities of βG and CBH decreased by 14.3–29.2% and 12.7–30.5% in the 10°-erosional plots, and 20.5–37.8% and 15.0–32.7% in the 20°-erosional plots ($p < 0.05$). However, βX showed no variation among the 5°-, 10°- and 20°-erosional plots. When compared to the 5°-depositional plot, the βX, βG and CBH activities increased by 2.2–13.5%, 20.6–28.9% and 33.8–54.8% in the 10°-depositional plot, respectively. The C-acquiring enzymes activities were enhanced by 10.0–18.1%, 17.3–32.1% and 14.8–86.2% in the 20°-depositional plot ($p < 0.05$, Fig. 2).

Table 2
Erosional responses for three slope gradients from 2016 to 2018.

Year	Annual rainfall (mm)	Annual erosion events	Slope (°)	Runoff (m^3)	Sediment yield (kg)	Erosion rate (t km^{-2} yr^{-1})
2016	524	10	5	0.27	14	2824
			10	0.58	45	8939
			20	0.58	48	9624
2017	560	16	5	0.23	2	423
			10	0.30	13	2549
			20	0.34	16	3159
2018	586	17	5	0.30	7	1489
			10	0.39	18	3632
			20	0.48	27	5499

Note: annual erosion events were the combined occurrence of runoff generation and sediment deposition per year (the data of 2016 and 2017 were cited from Du et al. (2020)).

3.3. Soil CO_2 emissions in the erosional and the depositional plots

During the experimental period of 2016–2018, the annual cumulative soil CO_2 emission appeared to significantly decrease by 20–41 g CO_2-C m^{-2} y^{-1} and 37–47 g CO_2-C m^{-2} y^{-1} in the 10°- and 20°-erosional plots compared to that in the 5°-erosional plots (288–329 g CO_2-C m^{-2} y^{-1}). Compared to the 5°-depositional plots (308–360 g CO_2-C m^{-2} y^{-1}), the cumulative soil CO_2 emission increased by 3–19 g CO_2-C m^{-2} y^{-1} and 25–42 g CO_2-C m^{-2} y^{-1} in the 10°- and 20°-depositional plots. Furthermore, total soil CO_2 emissions decreased with increasing slope gradients (Table 4).

3.4. Responses of soil C-acquiring enzyme activities to environmental variables and their controlling effects on soil CO_2 emissions

The SEM model showed a good fit between runoff, sediment, soil properties and C-acquiring enzyme activities ($\chi^2 = 0.984$, $p = 0.473$; RMSEA = 0.000, $p = 0.614$; standardized path coefficients are shown in Fig. 3). The results showed that the displaced runoff can affect the activities of βG and CBH by altering the soil moisture and DOC ($p < 0.05$). Meanwhile, the SOC, TN, clay, MBC and MBN were influenced by the sediment displacement, which influenced the enzyme activities of βX, βG and CBH ($p < 0.05$). In total, the model explained the 72%, 92% and 84% variances in βX, βG and CBH in the erosion–deposition plots, respectively (Fig. 3). Furthermore, the activities of βG and CBH in the erosional plots were positively correlated to the SOC, DOC, moisture, MBC and MBN while the βX activity was only affected by the clay. In the depositional plots, the SOC, microbial biomass and soil moisture influenced the C-acquiring enzymes βX and CHB activities, also the clay affected the βX activity; meanwhile, soil moisture and MBC were positively related to the βG activity (Table 5).

Moreover, the soil C-acquiring enzyme activities controlled the spatial variations of soil CO_2 emissions in the erosional and the depositional plots. Prominently, cumulative soil CO_2 emission linearly increased with the enzyme activities of βX, βG and CBH in the erosional

Table 3
Soil properties in the erosional plots and depositional plots across three slope gradients.

Year	Soil properties	Erosional plots			Depositional plots		
		5°	10°	20°	5°	10°	20°
2016	SOC (g kg^{-1})	8.70 ± 0.06B	8.43 ± 0.06A	8.39 ± 0.00A	8.70 ± 0.08a	8.87 ± 0.13a*	8.83 ± 0.12a*
	DOC (mg kg^{-1})	23.03 ± 0.40C	18.66 ± 1.09B	16.21 ± 0.89A	22.98 ± 1.39a	22.02 ± 2.69a*	22.15 ± 0.47a*
	N_{min} (mg kg^{-1})	1.84 ± 0.05B	1.86 ± 0.08B	1.52 ± 0.06A	2.26 ± 0.03a*	2.72 ± 0.16b*	2.53 ± 0.04b*
	TN (g kg^{-1})	0.73 ± 0.02A	0.73 ± 0.08A	0.76 ± 0.06A	0.68 ± 0.02a	0.79 ± 0.04b	0.79 ± 0.04b
	Moisture (m^3 m^{-3})	0.16 ± 0.00B	0.15 ± 0.00B	0.13 ± 0.01A	0.17 ± 0.00a	0.18 ± 0.00b*	0.20 ± 0.01c*
	MBC (mg kg^{-1})	129.25 ± 5.13B	111.30 ± 6.03A	113.06 ± 4.90A	144.80 ± 2.83a*	182.03 ± 5.84b*	180.46 ± 2.49b*
	MBN (mg kg^{-1})	6.54 ± 0.37C	5.24 ± 0.21B	4.30 ± 0.31A	12.84 ± 0.82a*	14.56 ± 0.46b*	17.56 ± 0.65c*
	Clay (%)	26.73 ± 0.49A	25.82 ± 0.38A	25.56 ± 0.53A	27.45 ± 0.22a	28.47 ± 0.39a*	28.17 ± 0.98a*
2017	SOC (g kg^{-1})	8.64 ± 0.02B	8.48 ± 0.01A	8.45 ± 0.03A	8.69 ± 0.07a	9.04 ± 0.09b*	8.97 ± 0.04b*
	DOC (mg kg^{-1})	23.28 ± 0.05B	22.35 ± 0.20AB	21.93 ± 0.44A	24.33 ± 0.52a*	26.09 ± 1.00a*	25.43 ± 0.49a
	N_{min} (mg kg^{-1})	1.83 ± 0.01C	1.68 ± 0.01B	1.53 ± 0.08Ab	2.59 ± 0.21a*	2.16 ± 0.17a*	2.44 ± 0.28a*
	TN (g kg^{-1})	0.77 ± 0.06A	0.74 ± 0.01A	0.72 ± 0.01A	0.74 ± 0.03a	0.78 ± 0.01a	0.77 ± 0.02a*
	Moisture (m^3 m^{-3})	0.17 ± 0.00B	0.15 ± 0.00AB	0.14 ± 0.01A	0.16 ± 0.01a	0.18 ± 0.01b*	0.19 ± 0.01b*
	MBC (mg kg^{-1})	148.45 ± 1.52C	123.15 ± 3.11B	112.40 ± 4.45A	135.49 ± 2.21a*	158.58 ± 5.03b*	181.52 ± 3.20c*
	MBN (mg kg^{-1})	7.12 ± 0.79B	6.01 ± 0.34AB	5.60 ± 0.37A	11.51 ± 1.07a*	14.51 ± 0.46b*	14.49 ± 0.66b*
	Clay (%)	26.12 ± 1.19A	24.68 ± 0.92A	24.93 ± 0.83A	24.04 ± 0.47a	26.68 ± 0.33b*	27.17 ± 0.97b
2018	SOC (g kg^{-1})	8.61 ± 0.11B	8.30 ± 0.02A	8.31 ± 0.04A	9.20 ± 0.32a*	9.19 ± 0.55a*	8.97 ± 0.75a
	DOC (mg kg^{-1})	22.33 ± 3.06A	21.54 ± 1.75A	18.38 ± 1.27A	20.08 ± 1.31a	20.79 ± 0.82a	20.18 ± 0.28a
	N_{min} (mg kg^{-1})	1.30 ± 0.13A	1.50 ± 0.14A	1.49 ± 0.05A	2.13 ± 0.09a*	2.73 ± 0.12b*	2.29 ± 0.46ab*
	TN (g kg^{-1})	0.69 ± 0.03A	0.68 ± 0.02A	0.69 ± 0.01A	0.78 ± 0.05a	0.73 ± 0.04a	0.74 ± 0.04a
	Moisture (m^3 m^{-3})	0.16 ± 0.00B	0.15 ± 0.01AB	0.14 ± 0.01A	0.17 ± 0.00a*	0.19 ± 0.00b*	0.20 ± 0.00c*
	MBC (mg kg^{-1})	132.40 ± 6.95B	124.58 ± 12.73AB	111.5 ± 36.61A	138.68 ± 14.52a	185.05 ± 13.75b*	185.89 ± 17.86b*
	MBN (mg kg^{-1})	6.98 ± 0.42C	5.08 ± 0.38B	3.66 ± 0.26A	15.9 ± 1.82a*	14.45 ± 0.66a*	14.6 ± 1.87a*
	Clay (%)	23.52 ± 0.49A	23.50 ± 0.76A	22.40 ± 1.27A	25.47 ± 0.59a*	26.13 ± 1.05a*	27.48 ± 1.34a*

Note: SOC, soil organic carbon; DOC, dissolved organic carbon; N_{min}, soil mineral nitrogen; TN, total nitrogen; MBC, soil microbial carbon biomass; MBN, soil microbial nitrogen biomass. Different capital letters indicate significant differences among the erosional plots, and different lowercase letters denote the difference among the depositional plots at $p < 0.05$, ANOVA, respectively. Asterisks represent significant differences between the erosional plots and the depositional plots at $p < 0.05$.

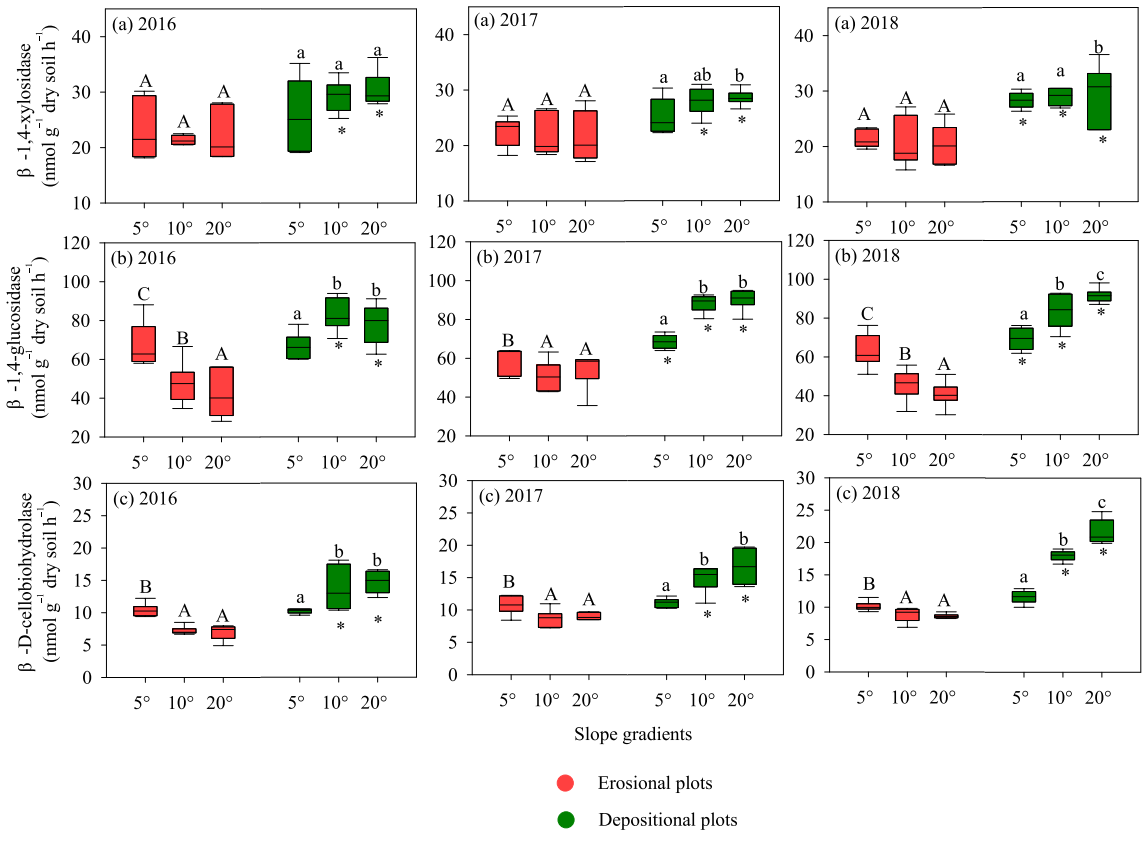

Fig. 2. The activities of β-1,4-xylosidase ((a) 2016, (a) 2017 and (a) 2018), β-1,4-glucosidase ((b) 2016, (b) 2017 and (b) 2018), and β-D-cellobiohydrolase ((c) 2016, (c) 2017 and (c) 2018)) in the erosional plots and the depositional plots across three slope gradients from 2016 to 2018. Different capital letters indicate significant differences among the erosional plots, and different lowercase letters denote the differences among the depositional plots, at $p < 0.05$ (ANOVA). Asterisks represent significant differences between the erosional plots and the depositional plots at $p < 0.05$.

Table 4
Soil cumulative CO_2 emission (g CO_2-C m^{-2} y^{-1}) in the erosional plots and the depositional plots and total soil CO_2 emission (g CO_2-C y^{-1}) in the whole erosion–deposition plots from 2016 to 2018.

Year	Soil cumulative CO_2 emission in the erosional plots			Soil cumulative CO_2 emission in the depositional plots			Total soil CO_2 emission		
	5°	10°	20°	5°	10°	20°	5°	10°	20°
2016	307 ± 16b	265 ± 19a	259 ± 4a	308 ± 39a	327 ± 36a	349 ± 11a*	1841 ± 115A	1653 ± 127A	1642 ± 29A
2017	329 ± 6c	309 ± 6b	292 ± 6a	360 ± 19a	371 ± 11a*	385 ± 21a*	2006 ± 48B	1914 ± 23AB	1845 ± 49A
2018	288 ± 5b	256 ± 5a	250 ± 2a	336 ± 6a*	340 ± 22a*	378 ± 3b*	1777 ± 22B	1620 ± 45A	1627 ± 12A

Different lowercase letters next to the values of soil cumulative CO_2 emission on the erosional plots denote significant differences among the 5°-, 10°- and 20°-erosional plots at $p < 0.05$. Different lowercase letters next to the values of soil cumulative CO_2 emission in the depositional plots denote significant differences among the 5°-, 10°- and 20°-depositional plots at $p < 0.05$. Different uppercase letters indicate the significant differences of total soil CO_2 emission among the erosion–deposition plots of 5°, 10° and 20°. Asterisks represent significant differences of soil cumulative CO_2 emission between the erosional plots and the depositional plots at $p < 0.05$. The total soil CO_2 emission was the sum of soil cumulative CO_2 emission in the 5 m^2 erosional plots and the 1 m^2 depositional plots yearly.

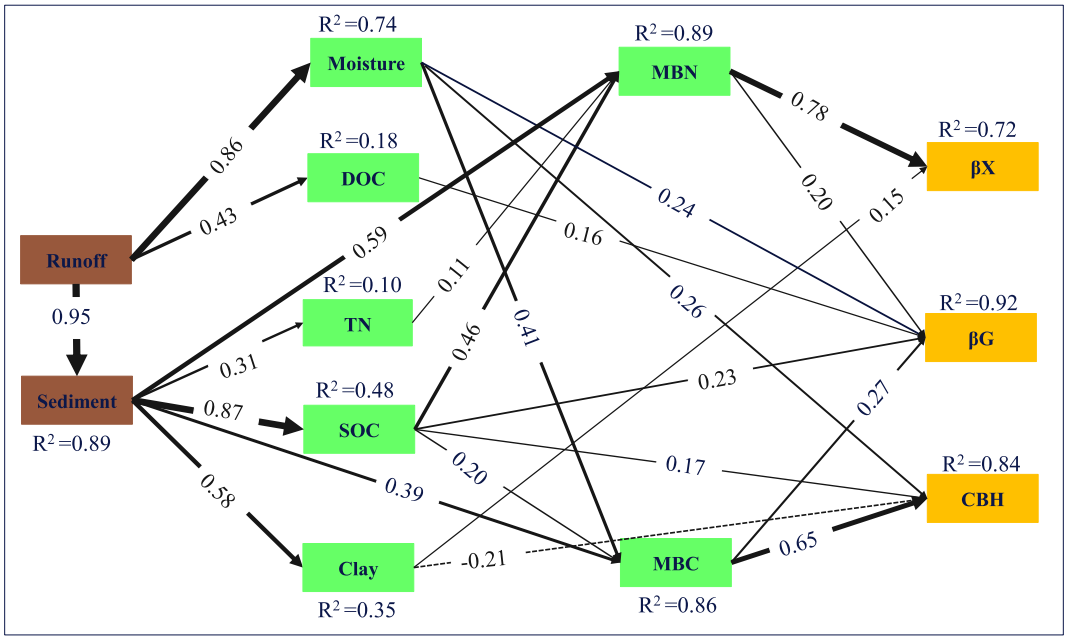

Fig. 3. Schematic representation of the path analyses used to identify the control of runoff and sediment displacement on C-acquiring enzyme activities. The black lines represent significant relationships at $p < 0.05$. The solid and dashed arrows indicate positive and negative relationships, respectively. The standardized path coefficients are embedded within the arrows. The arrow width is proportional to the strength of the path coefficients. R^2 indicates the proportion of variance explained and appears above every response variable in the model. The final model fit the data well: $\chi^2 = 1.101$, $p = 0.324$, RMSEA = 0.044, $p = 0.507$. SOC, soil organic carbon; DOC, dissolved organic carbon; TN, total nitrogen; MBC, soil microbial carbon biomass; MBN, soil microbial nitrogen biomass. βX, βG, and CBH represent β-1,4-xylosidase, β-1,4-glucosidase, β-D-cellobiohydrolase, respectively.

Table 5
Pearson correlations between soil C-acquiring enzyme activities and soil properties.

Soil properties	Erosional plots			Depositional plots		
	βX	βG	CBH	βX	βG	CBH
SOC	0.22	0.92**	0.71**	0.39*	0.33	0.40*
DOC	0.13	0.70**	0.75**	0.46*	0.12	–0.22
N_{min}	0.21	0.27	0.06	0.20	0.07	0.05
TN	0.17	0.12	–0.10	0.34	0.21	0.02
Moisture	–0.03	0.78**	0.60**	0.50**	0.69**	0.67**
MBC	0.05	0.71**	0.74**	0.63**	0.75**	0.78**
MBN	0.19	0.85**	0.67**	0.51**	0.29	0.30
Clay	0.40*	0.38	0.05	0.44*	0.33	0.23

Note: SOC, soil organic carbon; DOC, dissolved organic carbon; N_{min}, soil mineral nitrogen; TN, total nitrogen; MBC, soil microbial carbon biomass; MBN, soil microbial nitrogen biomass. The βX, βG, CBH represent β-1,4-xylosidase, β-1,4-glucosidase, β-D-cellobiohydrolase respectively. Significance levels are represented as '**' $p < 0.01$; '*' $p < 0.05$.

plots, and positively related to the βG and CBH in the depositional plots (Fig. 4, $p < 0.05$).

4. Discussion

4.1. Contrasting responses of the soil C-acquiring enzyme activities to erosion and deposition

The contrasting responses of soil C-acquiring enzyme activities, decreased in the erosional plots and increased in the depositional plots as the slope gradients steepened (Fig. 2), were mainly attributed to the runoff- and sediment-induced spatial distribution of the SOC, soil moisture, soil particles and microbial properties in the erosion–deposition plots (Table 3 and Fig. 3). Primarily, since the substrate supplement causes the microorganisms to secrete enzymes (Allison and Vitousek, 2005; Guo et al., 2018; Guo et al., 2019), the 1.9–3.6% SOC observed depletion with runoff and sediment displacement (Table 3) could account for the great proportion of the decreased enzyme activities in the 10°- and 20°-erosional plots relative to the 5°-erosional plots, confirmed by the positive effect of SOC on the activities of βG and CBH

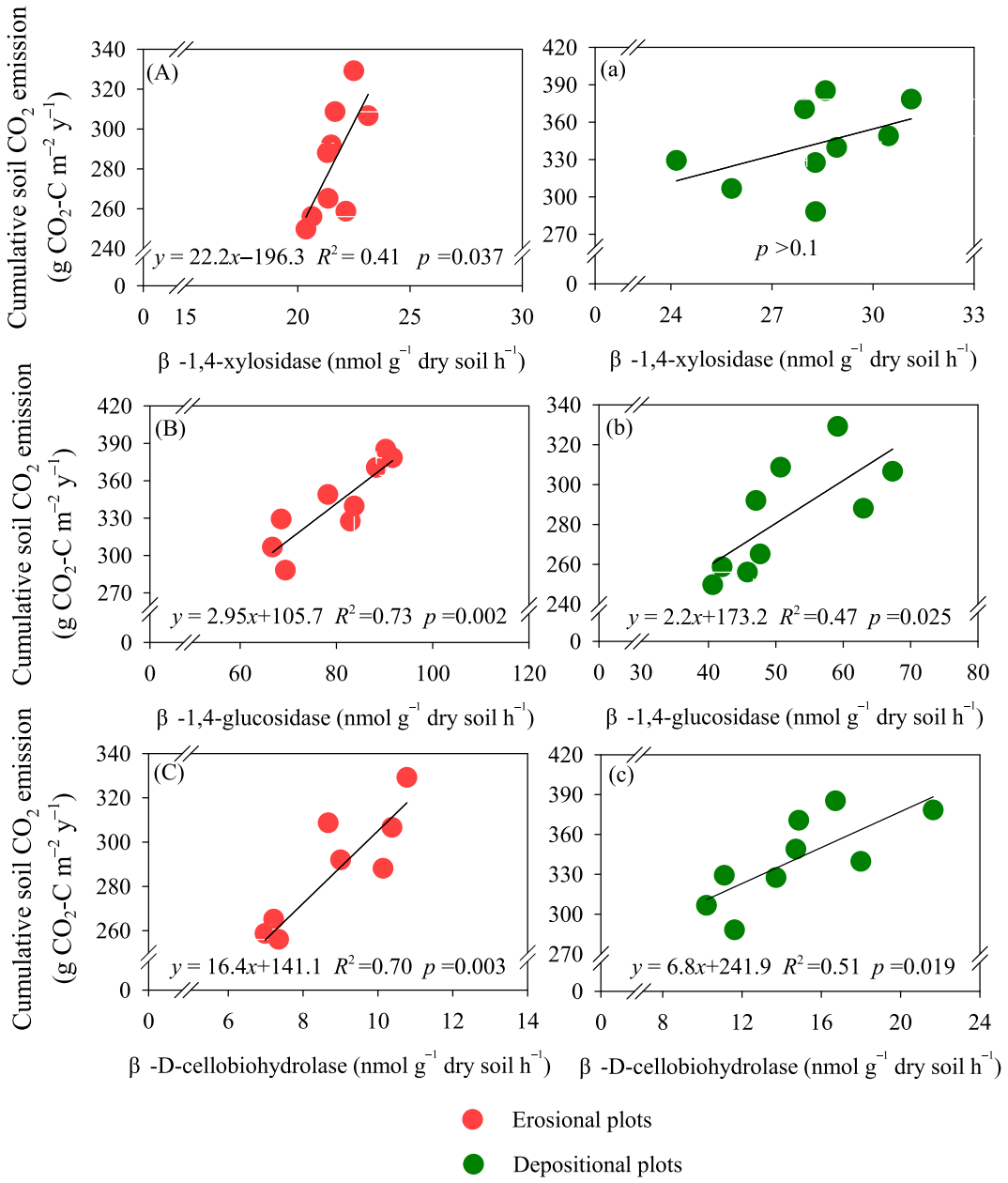

Fig. 4. Pearson correlations between the activities of β-1,4-xylosidase, β-1,4-glucosidase and β-D-cellobiohydrolase and the cumulative soil CO_2 emission in the erosional plots (A, B, C) and in the depositional plots (a, b, c).

(Fig. 3). A similar result was also observed by Moreno-de las Heras (2009), who reported that the exponential decreases in enzyme activities was in accordance with the depletion found in SOC. Conversely, the higher SOC concentration in the 10°- and 20°-depositional plots (Table 3) may enhance the enzyme activities through stimulating the microbial activity by the secretion of enzyme versus the lower SOC content supporting the lower enzyme activities in the 5-depositional plots. Furthermore, a lower microbial biomass was observed in the 10°- and 20°-erosional plots relative to that in the 5°-erosional plots (Table 3), which can probably cause a greater suppression on enzyme activities by down-regulating the amount of enzyme produced per unit of biomass (Waldrop et al., 2000). Meanwhile, due to the positive correlations between the enzyme activities and the MBC and MBN (Fig. 3), the more abundant microbial biomass in the 10°- and 20°-depositional plots relative to that in the 5°-depositional plots (Table 3) can be responsible for their higher enzyme activities. Additionally, because enzymes are easily absorbed on clay particle surfaces (Sollins et al., 1996), the removal of the clay also resulted in the removal of enzymes attached to the clay. Thus the clay particles selectively removed by runoff (Table 3) might play a role in reducing the enzyme activities of βG and CBH in the steeper erosional plots but have less effect on the βX activity in the erosional plots. Moreover, the soil moisture deficiency induced by runoff displacement in the erosional plots (Table 3) can decrease the enzyme activities of βG and CBH through increasing the enzyme immobilization and reducing the diffusion rates (Alster et al., 2013). It also might suppress the enzyme activities indirectly by inhibiting the available substrate diffusion for microbial production (Sardans and Peñuelas, 2005) or reducing the enzyme production of the microorganisms (Ali et al., 2015). The suppression effect of moisture deficiency on βG and CBH was more prominent in the 10°- and 20°-erosional plots than in the 5°-erosional plots. Conversely, soil moisture increased by 5.9–18.8% in the 10°- and 20°-depositional plots (Table 3) due to the input of runoff, which led to a positive effect on the soil C-acquiring enzyme activities (Fig. 3). This was consistent with the observation that

increasing soil moisture may highly enhance soil enzyme activities in semi-arid regions (Baldrian et al., 2013; Li et al., 2018). Notably, the βX activity showed less responses to the erosion-induced variations in soil environmental variables (Fig. 3 and Table 5). It suggested that the βX activity presented less sensitivity to soil erosion during the experimental period. Furthermore, although some of the βX enzyme was removed by runoff and sediment, the remaining βX, adsorbed onto particle surfaces, can still remain active to prevent enzyme activities from dropping severely (Allison and Vitousek, 2005). The βX adsorption producing enhanced enzyme activity (Tietjen and Wetzel, 2003) may compensate for the erosion-induced reduction in βX activity. Indeed, the active proportion of adsorbed βX might serve as a reservoir of potential enzyme activity during soil erosion process.

Contrary to the erosional plots, the depositional plots supported greater activities of the soil C-acquiring enzymes (Fig. 2). The runoff and sediment carried soil resources to be discharged into the depositional plots, which created more favourable soil conditions, with a higher moisture, nutrient content and microbial biomass (Table 3). Moreover, the carried or displaced soil resources may support greater enzyme activities and further stimulate higher microbial enzyme production compared to the erosional plots (Sardans and Peñuelas, 2005). The differences in soil C-acquiring enzyme activities between the erosional plots and the depositional plots increased in the steeper slope gradients of 10° and 20° relative to that difference in the 5° gentle slope (Fig. 2). The steeper slope gradients reinforced more runoff and sediment migration (Table 2) and enlarged the differences in the soil environment between the erosional plots and the depositional plots. Therefore, the larger variations in the environmental variables at the steeper slopes of 10° and 20° (Table 3) led to the greater differences in the soil C-acquiring enzyme activities between the erosional plots and the depositional plots. Our results confirmed that soil environmental heterogeneity exerted a critical control on the spatial distribution of soil C-acquiring enzyme activities in the eroding landscapes, consistent with previous studies (Li et al., 2015; Park et al., 2014; Sarapatka et al., 2018).

4.2. *The controlling effects of the soil C-acquiring enzymes on soil CO_2 emissions*

In this study, soil cumulative CO_2 emissions decreased in the erosional plots while increased in the depositional plots, which followed the spatial variations in the soil C-acquiring enzyme activities in the erosion–deposition plots (Table 4 and Fig. 2). These results suggested that soil C-acquiring enzyme activities performed their functions in soil CO_2 emissions during the erosion and deposition processes. It was evidenced by the positive linear relationships between the soil cumulative CO_2 emissions and the soil C-acquiring enzyme activities in both the erosional plots and the depositional plots (Fig. 4). These findings corresponded to previous studies of Allison and Vitousek (2005) and Mayes et al. (2012), which in that the SOC mineralization responses paralleled changes in the activities of the soil C-acquiring enzymes. Based on the contrasting variations in the soil CO_2 emissions controlled by the soil C-acquiring enzyme activities in the erosional plots and the depositional plots, the total soil CO_2 emissions from the entire erosion–deposition plot demonstrated a decreasing tendency as the slope gradients increased during 2016–2018 (Table 4). This indicated that the integrated changes in the soil C-acquiring enzyme activities in the erosional plots and the depositional plots were important in mitigating total soil CO_2 emissions in the erosion–deposition plots, which potentially contributes to the SOC sequestration in the eroding landscapes. Similarly, Mayes et al. (2012) demonstrated that a shrinking decrease in the enzyme activities contributed to the decreased CO_2 production and resulted in a greater stabilization of soil C. Our results emphasized the key role of the soil C-acquiring enzymes in controlling the SOC mineralization in the eroding landscape.

In this study, the activities of three soil C-acquiring enzymes showed highly sensitive responses to soil erosion and deposition, accompanied by changes in their function in mediating the soil C cycle. During the prolonged periods of erosion and deposition, the continued erosion of erosional plots transports material that originates from progressively deeper in the profile and deposited in a layered way on the lower depositional plots (Berhe et al., 2007). Such lateral and vertical redistribution of soil resources over a long time scale would accelerate the complexity in the spatial distribution of the soil C-acquiring enzyme activities. It may exert the disturbance on the stability of the soil C cycle in the eroding landscapes, resulting in a controlling effect of the soil C-acquiring enzymes on soil CO_2 emissions. Therefore, we should consider the variability of soil C-acquiring enzyme activities in assessing the effect of erosion and deposition on the soil C cycle.

5. Conclusion

The soil C-acquiring enzyme activities demonstrated contrasting responses to soil erosion and deposition. Specifically, the activities of the C-acquiring enzymes decreased with increasing soil erosion and increased with deposition. Remarkably, the activity of βX showed less sensitivity to soil erosion compared to βG and CBH. Furthermore, deposition stimulated higher soil C-acquiring enzyme activities than erosion, which was prominent on the steeper slopes. These spatial variations in the soil C-acquiring enzyme activities were triggered by the displaced runoff and sediment, and by their derived divergences in soil moisture, SOC, clay and microbial biomass. Moreover, the spatial distribution of the soil C-acquiring extracellular enzyme activities could contribute to SOC sequestration by decreasing the soil CO_2 emissions in the erosion–deposition plots. The spatial distribution of the C-acquiring enzyme activities and their controlling effects on soil CO_2 emissions provide evidence for determining the state and functionality of the soil system in the eroding landscape. Soil erosion and deposition in slope-scale involve the spatial translocation of soil particles in essential. As the important participant of soil erosion and deposition, eroded soil particles might contribute to the spatial variations of C-acquiring enzymes in different erosional and depositional plots. Understanding the activities of C-acquiring enzymes in particle-scale can help to reveal the influence mechanism of soil erosion and deposition on soil C-acquiring enzyme activities in the eroding landscapes. Therefore, the distribution patterns of the activities of C-acquiring enzymes in eroded particles should be given an investigation in future studies.

Declaration of Competing Interest

The authors declare that they have no known competing financial interests or personal relationships that could have appeared to influence the work reported in this paper.

Acknowledgements

This project was supported by the National Natural Science Foundation of China (No. 41371279).

Appendix A. Supplementary material

Supplementary data to this article can be found online at https://doi.org/10.1016/j.catena.2020.105047.

References

Ali, R.S., Ingwersen, J., Demyan, M.S., Funkuin, Y.N., Wizemann, H.-D., Kandeler, E., Poll, C., 2015. Modelling in situ activities of enzymes as a tool to explain seasonal variation of soil respiration from agro-ecosystems. Soil Biol. Biochem. 81, 291–303. https://doi.org/10.1016/j.soilbio.2014.12.001.

Ali, R.S., Kandeler, E., Marhan, S., Demyan, M.S., Ingwersen, J., Mirzaeitalarposhti, R., Rasche, F., Cadisch, G., Poll, C., 2018. Controls on microbially regulated soil organic

carbon decomposition at the regional scale. Soil Biol. Biochem. 118, 59–68. https://doi.org/10.1016/j.soilbio.2017.12.007.
Allison, S.D., Jastrow, J.D., 2006. Activities of extracellular enzymes in physically isolated fractions of restored grassland soils. Soil Biol. Biochem. 38 (11), 3245–3256. https://doi.org/10.1016/j.soilbio.2006.04.011.
Allison, S.D., Vitousek, P.M., 2005. Responses of extracellular enzymes to simple and complex nutrient inputs. Soil Biol. Biochem. 37, 937–944. https://doi.org/10.1016/j.soilbio.2004.09.014.
Alster, C.J., German, D.P., Lu, Y., Allison, S.D., 2013. Microbial enzymatic responses to drought and to nitrogen addition in a southern California grassland. Soil Biol. Biochem. 64, 68–79. https://doi.org/10.1016/j.soilbio.2013.03.034.
Baldrian, P., Šnajdr, J., Merhautová, V., Dobiášová, P., Cajthaml, T., Valášková, V., 2013. Responses of the extracellular enzyme activities in hardwood forest to soil temperature and seasonality and the potential effects of climate change. Soil Biol. Biochem. 56, 60–68. https://doi.org/10.1016/j.soilbio.2012.01.020.
Berhe, A.A., Barnes, R.T., Six, J., Marínspiotta, E., 2018. Role of soil erosion in biogeochemical cycling of essential elements: carbon, nitrogen, and phosphorus. Annu. Rev. Earth. Pl. Sc. 46 https://doi.org/10.1146/annurev-earth-082517-010018.
Berhe, A.A., Harte, J., Harden, J.W., Torn, M.S., 2007. The significance of the erosion-induced terrestrial carbon sink. Bioscience 57, 337–346. https://doi.org/10.1641/b570408.
Brockett, B.F.T., Prescott, C.E., Grayston, S.J., 2012. Soil moisture is the major factor influencing microbial community structure and enzyme activities across seven biogeoclimatic zones in western Canada. Soil Biol. Biochem. 44 (1) https://doi.org/10.1016/j.soilbio.2011.09.003.
Brookes, P.C., Landman, A., Pruden, G., Jenkinson, D.S., 1985. Chloroform fumigation and the release of soil nitrogen: A rapid direct extraction method to measure microbial biomass nitrogen in soil. Soil Biol. Biochem. 17, 837–842. https://doi.org/10.1016/0038-0717(85)90144-0.
Burns, R.G., DeForest, J.L., Marxsen, J., Sinsabaugh, R.L., Stromberger, M.E., Wallenstein, M.D., Weintraub, M.N., Zoppini, A., 2013. Soil enzymes in a changing environment: Current knowledge and future directions. Soil Biol. Biochem. 58, 216–234. https://doi.org/10.1016/j.soilbio.2012.11.009.
Conant, R.T., Ryan, M.G., Ågren, G.I., Birge, H.E., Davidson, E.A., Eliasson, P.E., Evans, S.E., Frey, S.D., Giardina, C.P., Hopkins, F.M., Hyvönen, R., Kirschbaum, M.U. F., Lavallee, J.M., Leifeld, J., Parton, W.J., Megan Steinweg, J., Wallenstein, M.D., Martin Wetterstedt, J.Å., Bradford, M.A., 2011. Temperature and soil organic matter decomposition rates - synthesis of current knowledge and a way forward. Global Change Biol. 17, 3392–3404. https://doi.org/10.1111/j.1365-2486.2011.02496.x.
de Nijs, E.A., Cammeraat, E.L.H., 2020. The stability and fate of Soil Organic Carbon during the transport phase of soil erosion. Earth-Sci. Rev. 201, 103067. https://doi.org/10.1016/j.earscirev.2019.103067.
Delgado-Baquerizo, M., García-Palacios, P., Milla, R., Gallardo, A., Maestre, F.T., 2015. Soil characteristics determine soil carbon and nitrogen availability during leaf litter decomposition regardless of litter quality. Soil Biol. Biochem. 81, 134–142. https://doi.org/10.1016/j.soilbio.2014.11.009.
Du, L.L., Wang, R., Gao, X., Hu, Y.X., Guo, S.L., 2020. Divergent responses of soil bacterial communities in erosion-deposition plots on the Loess Plateau. Geoderma 358, 113995. https://doi.org/10.1016/j.geoderma.2019.113995.
Grossman, R.B., Reinsch, T.G., 2002. 2.1 Bulk Density and Linear Extensibility, Methods of Soil Analysis: Part 4 Physical Methods. SSSA Book Series. Soil Science Society of America, Madison, WI, pp. 201–228.
Guo, Y., Chen, X., Wu, Y., Zhang, L., Cheng, J., Wei, G., Lin, Y., 2018. Natural revegetation of a semiarid habitat alters taxonomic and functional diversity of soil microbial communities. Sci. Total Environ. 635, 598–606. https://doi.org/10.1016/j.scitotenv.2018.04.171.
Guo, Y., Hou, L., Zhang, Z., Zhang, J., Cheng, J., Wei, G., Lin, Y., 2019. Soil microbial diversity during 30 years of grassland restoration on the Loess Plateau, China: Tight linkages with plant diversity. Land Degrad. Dev. 30, 1172–1182. https://doi.org/10.1002/ldr.3300.
Hu, Y., Kuhn, N.J., 2016. Erosion-induced exposure of SOC to mineralization in aggregated sediment. Catena 137, 517–525. https://doi.org/10.1016/j.catena.2015.10.024.
Kjeldahl, J., 1883. Neue Methode zur Bestimmung des Stickstoffs in organischen Körpern. Anal. Bioanal. Chem. 22, 366–382. https://doi.org/10.1007/BF01338151.
Kuhn, N.J., Hoffmann, T., Schwanghart, W., Dotterweich, M., 2009. Agricultural soil erosion and global carbon cycle: controversy over? Earth Surf. Proc. Land. 34, 1033–1038. https://doi.org/10.1002/esp.1796.
Lal, R., 2019. Accelerated Soil erosion as a source of atmospheric CO_2. Soil Till. Res. 188, 35–40. https://doi.org/10.1016/j.still.2018.02.001.
Li, G.L., Kim, S., Han, S.H., Chang, H.N., Du, D.L., Son, Y., 2018. Precipitation affects soil microbial and extracellular enzymatic responses to warming. Soil Biol. Biochem. 120, 212–221. https://doi.org/10.1016/j.soilbio.2018.02.014.
Li, Z.W., Xiao, H.B., Tang, Z.H., Huang, J.Q., Nie, X.D., Huang, B., Ma, W.M., Lu, Y.M., Zeng, G.M., 2015. Microbial responses to erosion-induced soil physico-chemical property changes in the hilly red soil region of southern China. Eur. J. Soil Bio. 71, 37–44. https://doi.org/10.1016/j.ejsobi.2015.10.003.
Mayes, M.A., Post, W.M., Wang, G., Jagadamma, S., Steinweg, J.M., Schadt, C.W., 2012. Developing an enzyme mediated soil organic carbon decomposition model. https://doi.org/2012AGUFM.B33C0531M.
Mccarty, G.W., Ritchie, J.C., 2002. The Impact of soil movement on carbon sequestration in agricultural ecosystems. Environ. Pollut. 116, 423–430. https://doi.org/10.1016/S0269-7491(01)00219-6.
Moreno-de las Heras, M., 2009. Development of soil physical structure and biological functionality in mining spoils affected by soil erosion in a Mediterranean-Continental environment. Geoderma 149, 249–256. https://doi.org/10.1016/j.geoderma.2008.12.003.
Nie, X., Zhang, J., Gao, H., 2015. Soil enzyme activities on eroded slopes in the Sichuan Basin, China. Pedosphere 25, 489–500. https://doi.org/10.1016/s1002-0160(15)30030-8.
Park, J.H., Meusburger, K., Jang, I., Kang, H., Alewell, C., 2014. Erosion-induced changes in soil biogeochemical and microbiological properties in Swiss Alpine grasslands. Soil Biol. Biochem. 69, 382–392. https://doi.org/10.1016/j.soilbio.2013.11.021.
Peng, X.Q., Wang, W., 2016. Stoichiometry of soil extracellular enzyme activity along a climatic transect in temperate grasslands of northern China. Soil Biol. Biochem. 98, 74–84. https://doi.org/10.1016/j.soilbio.2016.04.008.
Polyakov, V.O., Lal, R., 2008. Soil organic matter and CO_2 emission as affected by water erosion on field runoff plots. Geoderma 143, 216–222. https://doi.org/10.1016/j.geoderma.2007.11.005.
Sagova-Mareckova, M., Zadorova, T., Penizek, V., Omelka, M., Tejnecky, V., Pruchova, P., Chuman, T., Drabek, O., Buresova, A., Vanek, A., Kopecky, J., 2016. The structure of bacterial communities along two vertical profiles of a deep colluvial soil. Soil Biol. Biochem. 101, 65–73. https://doi.org/10.1016/j.soilbio.2016.06.026.
Saiya-Cork, K.R., Sinsabaugh, R.L., Zak, D.R., 2002. The effects of long term nitrogen deposition on extracellular enzyme activity in an Acer saccharum forest soil. Soil Biol. Biochem. 34, 1309–1315. https://doi.org/10.1016/S0038-0717(02)00074-3.
Sarapatka, B., Cap, L., Bila, P., 2018. The varying effect of water erosion on chemical and biochemical soil properties in different parts of Chernozem slopes. Geoderma 314, 20–26. https://doi.org/10.1016/j.geoderma.2017.10.037.
Sardans, J., Peñuelas, J., 2005. Drought decreases soil enzyme activity in a Mediterranean Quercus ilex L. forest. Soil Biol. Biochem. 37, 455–461. https://doi.org/10.1016/j.soilbio.2004.08.004.
Sinsabaugh, R.L., Lauber, C.L., Weintraub, M.N., Ahmed, B., Allison, S.D., Crenshaw, C., Contosta, A.R., Cusack, D., Frey, S., Gallo, M.E., Gartner, T.B., Hobbie, S.E., Holland, K., Keeler, B.L., Powers, J.S., Stursova, M., Takacs-Vesbach, C., Waldrop, M. P., Wallenstein, M.D., Zak, D.R., Zeglin, L.H., 2008. Stoichiometry of soil enzyme activity at global scale. Ecol. Lett. 11, 1252–1264. https://doi.org/10.1111/j.1461-0248.2008.01245.x.
Sollins, P., Homann, P., Caldwell, B.A., 1996. Stabilization and destabilization of soil organic matter: mechanisms and controls. Geoderma 74, 65–105. https://doi.org/10.1016/S0016-7061(96)00036-5.
Sparks, D.L., Page, A.L., Helmke, P.A., Loeppert, R.H., Soltanpour, P.N., Tabatabai, M.A., Johnston, C.T., Sumner, M.E., 1996. Methods of Soil Analysis. Part 3 - Chemical Methods. SSSA Book Series 5. Soil Science Society of America Journal, Madison.
Stallard, R.F., 1998. Terrestrial sedimentation and the carbon cycle: Coupling weathering and erosion to carbon burial. Global Biogeochem. Cy. 12, 231–257. https://doi.org/10.1029/98gb00741.
Starr, G.C., Lal, R., Kimble, J.M., Owens, L., 2001. Assessing the impact of erosion on soil organic carbon pools and fluxes. In: Lal, R., Kimble, J.M., Follet, R.F., Stewart, B.A. (Eds.), Assessment Methods for Soil Carbon. Lewis, Boca Raton, FL, pp. 417–426.
Tietjen, T., Wetzel, R.G., 2003. Extracellular enzyme-clay mineral complexes: Enzyme adsorption, alteration of enzyme activity, and protection from photodegradation. Aquat. Ecol. 37, 331–339. https://doi.org/10.1023/B:AECO.0000007044.52801.6b.
Van Oost, K., Quine, T.A., Govers, G., De Gryze, S., Six, J., Harden, J.W., Ritchie, J.C., McCarty, G.W., Heckrath, G., Kosmas, C., Giraldez, J.V., da Silva, J.R.M., Merckx, R., 2007. The impact of agricultural soil erosion on the global carbon cycle. Science 318, 626–629. https://doi.org/10.1126/science.1145724.
Vance, E.D., Brookes, P.C., Jenkinson, D.S., 1987. An extraction method for measuring soil microbial biomass C. Soil Biol. Biochem. 19, 703–707. https://doi.org/10.1016/0038-0717(87)90052-6.
Waldrop, M.P., Balser, T.C., Firestone, M.K., 2000. Linking microbial community composition to function in a tropical soil. Soil Biol. Biochem. 32, 1837–1846. https://doi.org/10.1016/S0038-0717(00)00157-7.
Wang, Z.Q., Hu, Y.X., Wang, R., Guo, S.L., Du, L.L., Zhao, M., Yao, Z.H., 2017. Soil organic carbon on the fragmented Chinese Loess Plateau: Combining effects of vegetation types and topographic positions. Soil Till. Res. 174, 1–5. https://doi.org/10.1016/j.still.2017.05.005.
Wei, S.C., Zhang, X.P., McLaughlin, N.B., Yang, X.M., Liang, A.Z., Jia, S.X., Chen, X.W., 2016. Effect of breakdown and dispersion of soil aggregates by erosion on soil CO_2 emission. Geoderma 264, 238–243. https://doi.org/10.1016/j.geoderma.2015.10.021.
Xiao, H.B., Li, Z.W., Chang, X.F., Huang, B., Nie, X.D., Liu, C., Liu, L., Wang, D.Y., Jiang, J.Y., 2018. The mineralization and sequestration of organic carbon in relation to agricultural soil erosion. Geoderma 329, 73–81. https://doi.org/10.1016/j.geoderma.2018.05.018.
Xu, Z.W., Yu, G.R., Zhang, X.Y., He, N.P., Wang, Q.F., Wang, S.Z., Wang, R.L., Zhao, N., Jia, Y.L., Wang, C.Y., 2017. Soil enzyme activity and stoichiometry in forest ecosystems along the North-South Transect in eastern China (NSTEC). Soil Biol. Biochem. 104, 152–163. https://doi.org/10.1016/j.soilbio.2016.10.020.
Zhang, Y.J., Guo, S.L., Liu, Q.F., Jiang, J.S., Wang, R., Li, N.N., 2015. Responses of soil respiration to land use conversions in degraded ecosystem of the semi-arid Loess Plateau. Ecol. Eng. 74, 196–205. https://doi.org/10.1016/j.ecoleng.2014.10.003.